

Fabrication and Fatigue Testing of an Electrostatically Driven Microcantilever Beam

Y. C. LIN, H. HOCHENG, W. L. FANG, AND R. CHEN

Department of Power Mechanical Engineering, National Tsing Hua University, Hsinchu, Taiwan, R.O.C.

The reliability of a microelectromechanical system is an essential issue before the microdevice can be applied in practice. It is indispensable to investigate the mechanical properties of a microstructure to meet the requirements for longer lifetime and reliable performance. This paper studies the fabrication and the fatigue characteristics of a microcantilever beam, which is among the most widely employed microstructures in sensors and actuators. A pad is fabricated at the free end of the beam for larger effective external electrostatic load on the specimen. In fatigue tests, the specimen is actuated by the electrical voltage of 150 and 200 V at 100 Hz. The deflection of the beam is measured by the laser Doppler vibrometer. Based on the experimental results and ANSYS calculation, the displacement of the free end of the beam increases with the beam length and the applied load, and ranges from 61 to 600 nm. The fatigue life lies between 6.1×10^6 and 1.4×10^8 cycles. These results are consistent with the reference of a microcantilever beam subject to magnetic load.

Keywords Electrostatic; Fatigue; MEMS; Microcantilever beam; Reliability.

INTRODUCTION

Knowledge of the material properties is important for the design of a novel device in microelectromechanical systems (MEMS). There is no well-established code for testing the material characteristics in consideration of the fabrication processes [1]. Recently, many researchers have been devoted to investigating the mechanical properties of the microcantilever beams by various approaches, such as the tensile test [2–7], bending test [3, 8], and fatigue test [9–16]. In the fatigue test, there are several methods to tell the fatigue occurrence, including the stress amplitude [9, 10, 13, 16], the variation of the stiffness [12, 14–16], and the change of the resonant frequency [9, 13, 16] as discussed below.

Muhlstein, Brown, and Ritchie used the electrostatic comb drive actuator to apply the load to a notched cantilever beam, which is attached to a large, perforated plate that serves as a resonant mass [9]. The geometry of the beam made of single crystal silicon was 40 μm in length, 21.5 μm in width, and 20 μm in height. The testing frequency was 40 and 50 kHz. The results showed that the fatigue life in swinging motion ranged from about 10s to 48 days, or 1×10^6 to 1×10^{11} cycles before failure. The fatigue of the polycrystalline silicon was also investigated by the same actuation method. The longer releasing time may lead to higher resonant frequency and longer lifetime of the device [13].

Resonant frequency was also used to indicate the fatigue life of the specimen. The drift of the resonant frequency in fact shows the growth of the microdefect in a device. Muhlstein, Brown, and Ritchie observed that the resonant frequency decayed with time due to the progressive decrease

in stiffness of the beam [9, 13]. Schwaiger and Kraft studied the fatigue behavior of various Ag film thicknesses on the SiO_2 cantilever beam. The beam specification was 30–50 μm long, 10 μm wide, 2.83 μm thick, coated by a 0.2–1.5- μm -thick Ag film. The applied force ranged from 40 to 800 μN at 45 Hz. The mean stress levels ranged from 126 to 600 MPa and the 1.5 μm Ag film damage was consistently observed after 3×10^6 cycles. Thinner films were more fatigue resistant and contained fewer and smaller extrusions than thicker films [10]. Ando, Shikida, and Sato performed a tensile-mode fatigue testing of silicon films. The testing specimen was made of single-crystal-silicon 50 μm long, 50 μm wide, and 5 μm thick. The loads ranging from 10–130 mN were applied by a needle at a frequency of 10 Hz. The fracture of the specimen was determined by the output signal from the load cell as a function of time. The load rapidly dropped down at the fracture. The fracture occurred at about 10^5 cycles [11].

Stiffness was also a factor adopted to define the fatigue life of the specimen. Stiffness decreased when fracture occurred at the interior of the structure [12, 14–16]. Li and Bhushan used the nanoindenter to apply an oscillating load on a double clamped Si beam. The beam was 600 nm in length, 380 nm in upper width, 790 nm in lower width, and 255 nm in thickness. It was deflected by the sinusoidal load with amplitude of 25 μN , mean load of 100 μN , and frequency of 45 Hz. In their study, the sharp decrease in contact stiffness indicated that the fatigue damage was produced [12, 14–16] approximately at 0.6×10^4 cycles [12].

Based on previous research [2–16], most of the investigations on material properties, including fatigue analysis, were performed with testing methods using low frequency loading in contact with the specimen. The experimental results, however, varied with the testing equipment, such as the probe. The loading frequency was limited between 45–60 Hz due to the structure response of the testing device.

Received October 13, 2004; Accepted January 25, 2005

Address Correspondence to H. Hocheng, Department of Power Mechanical Engineering, National Tsing Hua University, Hsinchu 300, Taiwan, R.O.C.; E-mail: hocheng@pme.nthu.edu.tw

Noncontact testing methods using magnetic or electrostatic actuations can be used to avoid contact disturbance during a test, such as slipping problems [8]. Hence, it is feasible to work at a higher frequency, simulating the actual operation up to the kilohertz of the MEMS component. The magnetic load, however, was often found dramatically affected by the heat generated in the magnetic circuit [17]. Instead, the electrostatic force is easy to control and is relatively stable. Besides, an electrostatically driven actuator not only provides high-frequency response but also consumes less power, and is easy to fabricate [18]. This paper presents the fabrication method and the fatigue of the polysilicon microcantilever beams driven by the electrostatic load as a reference to the reliability design for MEMS.

DESIGN AND FABRICATION OF SPECIMEN

Specimen Design

The specimen consists of a beam body and two pads, as shown in Fig. 1. Pad #1 is used to fix the sample on the electrode where the voltage is transmitted to the specimen. Compared to the beam body, Pad #1 is large and wide. Therefore, little residual stress will be produced in this structure. Pad #2 is located at the other end of the cantilever beam for the generation of large electrostatic

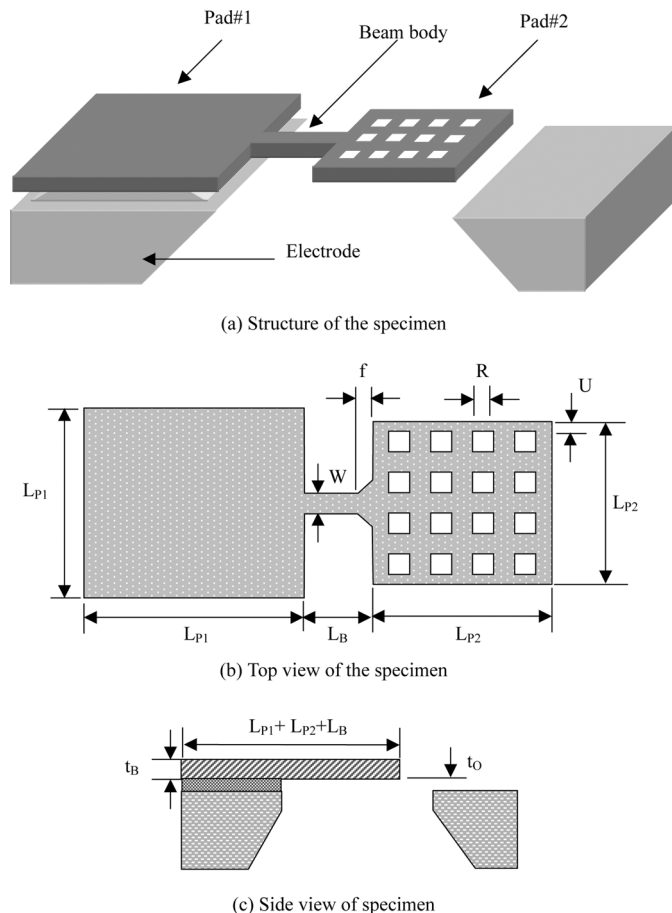


FIGURE 1.—Design of specimen.

TABLE 1.—Dimensions of specimen.

Parameters	Values (μm)	Parameters	Values (μm)
L_{P1}	1000	R	20
L_B	60, 80, 100, 120	U	20
L_{P2}	500, 560	t_B	2
W	20	t_O	1
f	20		

loads. Compared to the size of the beam, the electrostatic load generated by Pad #2 is much larger than that on the beam. The electrostatic load generated by the cantilever beam can be neglected. The perforations in Pad #2 are applied for reducing the air damping effect when the beam structure vibrates. Pad #2 serves also for the convenient measurement of the beam deflection. Owing to the tiny size of the cantilever beam, it is difficult to align the measuring laser and the specimen during the fatigue test. Additionally, a special fillet design is developed at the connection between the beam body and Pad #2 to ensure that the neck will not fail before the beam root at the fixed end does. The dimension design of specimen are shown in Table 1.

Fabrication Processes

The fabrication processes, including deposition, doping, annealing, lithography, etching, etc., are developed as follows. First, a layer of $1\mu\text{m}$ wet oxide is grown on both sides of the silicon substrate in the furnace [Fig. 2(a)]. The polysilicon of the structure layer is then deposited by low pressure chemical vapor deposition (LPCVD) above the oxide to $2\mu\text{m}$ thick [Fig. 2(b)]. In order to reduce the resistivity of the polysilicon and to ensure that the specimen can be actuated in an electrostatic field, the *n*-typed doping process is performed in POCl_3 at 1050° for 30 minutes following the polysilicon deposition [Fig. 2(c)]. Due to the importance of the elimination of the residual stress, the polysilicon is annealed in a nitrogen environment at 1050° for 60 minutes to avoid failure of the specimen after release [Fig. 2(d)]. The geometry of the structure is defined by the lithography techniques with mask A [Fig. 2(m)] and reactive ion etching (RIE) [Fig. 2(e)]. The passivation layer of silicon nitride against TMAH attack is deposited over the polysilicon by LPCVD to 2000 \AA thick [Fig. 2(f)]. Furthermore, for better protection of the structures against TMAH etchant, a layer of $5\mu\text{m}$ thick PECVD TEOS oxide deposited on the nitride film can ensure the specimens surviving after a long period of wet etching [Fig. 2(g)]. In consideration of the TMAH property for high selectivity between silicon, and thermal oxide and nitride, the etching rate of TMAH 22% wt. at 80° is $32\mu\text{m/hr}$ for silicon, 0.00054g for oxide, and nearly 0 for nitride [19–22]. On the backside of the wafer, mask B [Fig. 2(n)] is applied to open the windows on the etching mask layers, the oxide and nitride [Fig. 2(h)]. Hence, the substrate can be patterned by TMAH etching according to the definition of these windows without damage to the front side structures [Fig. 2(i)]. As a $70\text{-}\mu\text{m}$ -thick membrane is created, the oxide and nitride on the front side is stripped by concentrated HF (49%) and RIE, respectively, in order to eliminate the negative effect

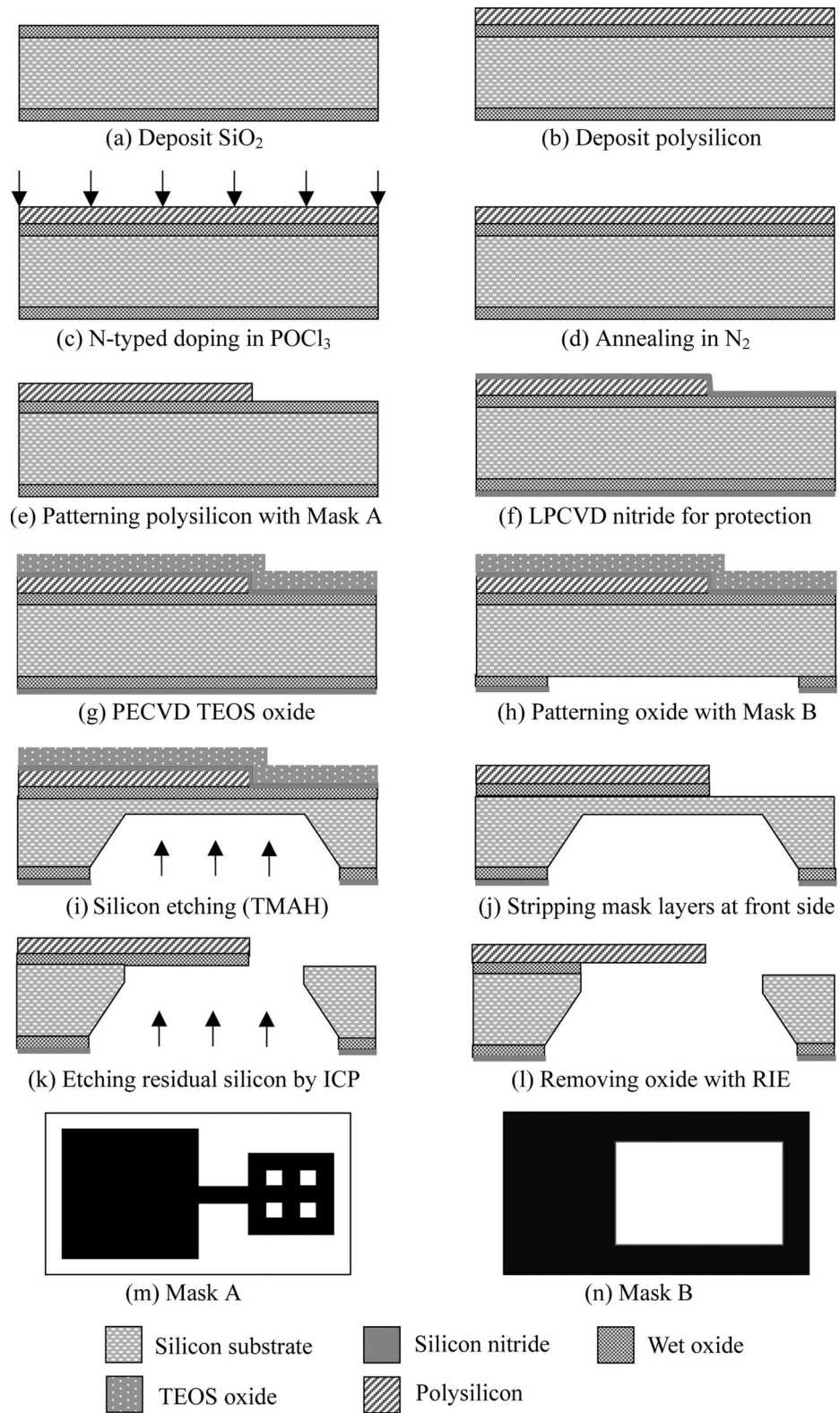


FIGURE 2.—Fabrication processes of specimen.

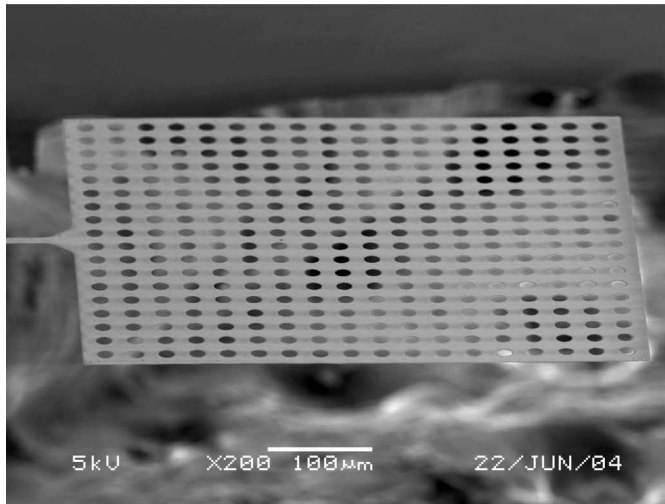
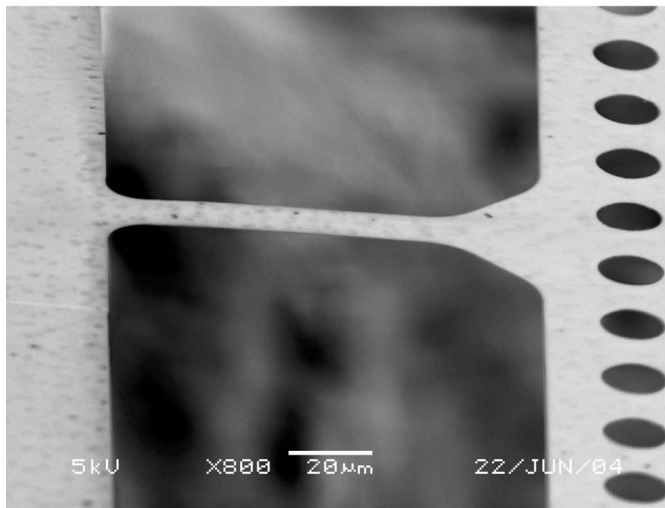
(a) Pad #2 of 560 $\mu\text{m} \times 560 \mu\text{m}$ (b) Beam body of 100 $\mu\text{m} \times 20 \mu\text{m}$

FIGURE 3.—Fabricated specimen.

of the residual stress of the oxide and nitride on the structure layer [Fig. 2(j)]. The silicon membrane is then removed by inductive coupling plasma etching (ICP), which not only obtains better uniformity and stops etching at the oxide layer, but also avoids damage caused by the turbulence generated by stirring and surface tension in the wet etchant [Fig. 2(k)]. (The selectivity between silicon and wet oxide is approximately 120:1). Finally, after the oxide layer is removed from the backside with RIE, the desired specimen is produced [Fig. 2(l)]. The fabricated specimen is shown in Fig. 3.

EXPERIMENTAL SETUP OF BEAM FATIGUE

The testing and measuring setup consists of the function generator, the power amplifier, the probe, the electrode, the laser displacement meter, and the optical microscope,

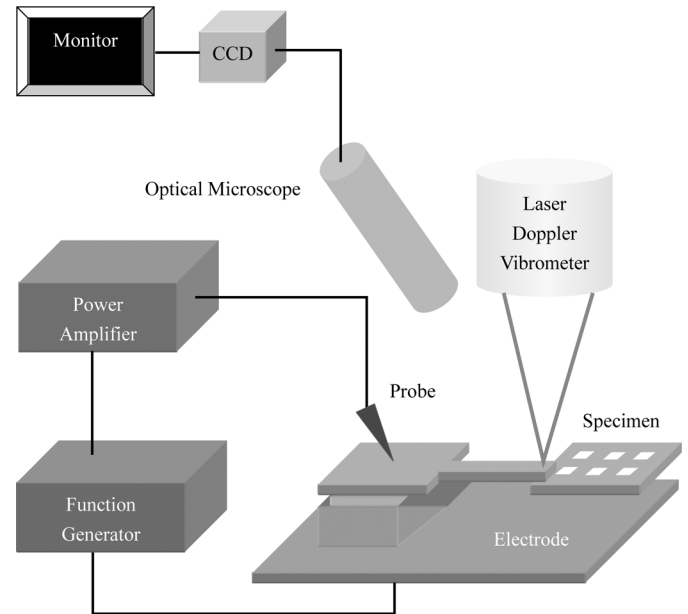


FIGURE 4.—Experimental setup.

as elaborated in Fig. 4. In the actuation module, the function generator (Hewlett Packard 33120A) and the power amplifier (NF Electronic Instruments 4010) are used to produce the electrostatic load at a certain frequency on the specimen. In this study, the digital wave (100 Hz), which is much less than the resonant frequency (shown in Table 2) to avoid the resonance effect, is generated by the function generator. The voltage output from the generator is magnified by the power amplifier (150 and 200 V in the current test). Additionally, the electrode is made of pure copper with excellent conductivity. At the voltage difference across the specimen and the copper plate, the electrostatic load is generated following the frequency of the function generator. The beam under load deflects and vibrates accordingly. The magnitude of the electrostatic load is determined by the overlapped area between the specimen and the copper plate (100 cm^2) and the distance in between ($525 \mu\text{m}$). The electrostatic load is estimated $2.9\text{--}5.2 \times 10^{-4} \text{ N}$.

In the measurement module, the data of the deflection of the specimen is obtained by a laser Doppler vibrometer (Polytec MSV 400). The setup of the laser doppler vibrometer (LDV) is shown in Fig. 5. For out-of-plane motions, the measurement resolution is in the range of a picometer. An optical microscope is applied to align the laser beam and the specimen precisely. The displacement data can be obtained accurately for later calculation of the stress distribution.

TABLE 2.—Resonant frequency of the testing specimens.

L_B (μm)	Pad #2 = $500 \times 500 \mu\text{m}^2$	Pad #2 = $560 \times 560 \mu\text{m}^2$
60	2835.8 Hz	2290.8 Hz
80	2434.9 Hz	1958.1 Hz
100	2142.4 Hz	1728.9 Hz
120	1916.7 Hz	1551.8 Hz

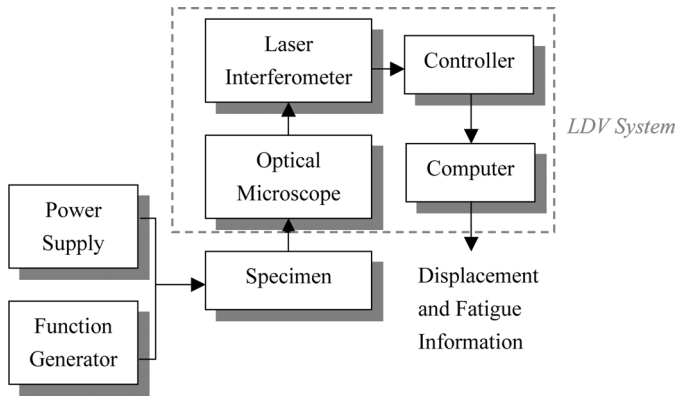


FIGURE 5.—Setup of laser Doppler vibrometer.

The fatigue test conditions are as follows. The gap between the specimen and the electrode is 525 μm. The applied voltages for the electrostatic load are 150 and 200 V in digital wave at 100 Hz. The resonant effect can be neglected because the actuation frequency, 100 Hz, is much lower than the resonant frequency of the specimens. The total testing time is 422.15 hours, namely the maximum deflection cycle is about 1.52×10^8 .

RESULTS AND DISCUSSIONS

The displacement of all specimens in the first 20 minutes are sampled and averaged, as shown in Fig. 6. The factors affecting the displacement are the applied voltage and the beam length. The deflection increases with these factors significantly. The neck deflection ranges from 61 nm to 460 nm at 150 V and from 320 nm to 600 nm at 200 V.

Based on the observation in the experiment, the specimen does not break through the cross-section of specimen when fatigue occurs. Instead, the cantilever beam deflects so severely that the pad makes contact with the electrode. Although no obvious defects appear on the specimen, the specimen cannot resume its normal deflection behavior in

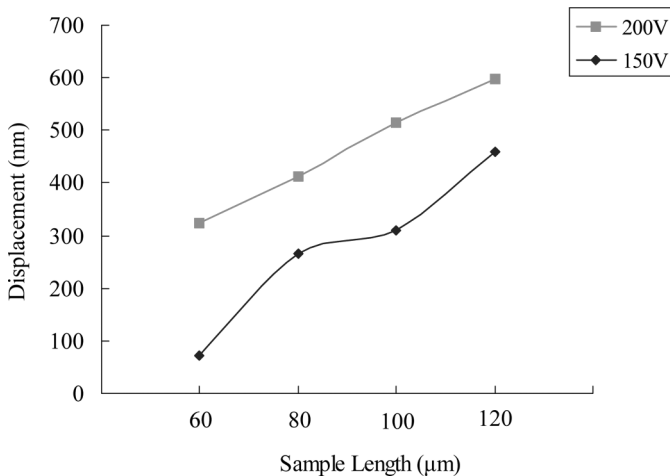


FIGURE 6.—Neck displacement in Z direction.

the electrostatic field. The microcantilever beam normally vibrates according to the applied frequency and the voltage. It can be used as a switch to transmit the electrical signal. When its motion cannot continue to pass the input signal, the component is defined as failure (or fatigue). The beam cannot resume its normal deflection because the stiffness decreases with the internal material damage. The specimen is then examined by Scanning electron microscopy (SEM). The fatigue life data of the specimens are summarized in Table 3. It is found that the fatigue rate of the longest specimen, 120 μm, is the highest. More long samples fail at shorter cycles, while the short beam fails later at a larger number of cycles. This rate also increases when the applied electrical load is increased from 150 V to 200 V. It is attributed to the increased stress in the beam. The fatigue behavior of the specimens will vary with the fabrication conditions, such as the doping concentration, the deposition uniformity, and the etching quality. These conditions change the microscopic material characteristics. Hence, a code for the fabrication should be constructed in the future for industrial tests.

The average fatigue life is calculated by the weighted average method

$$n_{avg} = \frac{\sum_{x=1}^k n_x w_x}{\sum_{x=1}^k w_x} \tag{1}$$

TABLE 3.—Number of failed samples at various beam lengths.

Cycles ($\times 10^6$)	60 μm	80 μm	100 μm	120 μm
(a) 150 V				
6.12	0	0	0	0
9.36	0	0	0	0
15.0	0	0	2	15
18.24	0	0	0	6
34.74	0	0	0	0
43.62	0	0	0	2
45.78	0	0	0	0
61.44	0	0	0	0
70.38	0	0	3	1
87.24	0	0	0	0
96.12	0	0	1	0
Total failed	0	0	6	24
Total samples	2	1	31	29
Fatigue rate (%)	0	0	19.35	82.76
(b) 200 V				
7.452	0	0	1	2
11.16	0	0	1	5
11.88	0	0	0	8
12.6	0	0	1	15
12.96	0	0	1	5
13.86	0	1	0	0
15.66	0	1	3	4
17.68	0	1	1	2
30.98	0	0	0	2
32.35	0	0	0	0
47.14	0	0	0	1
81.71	0	0	0	1
113.2	0	0	2	0
141.4	0	0	2	0
Total failed	0	3	12	45
Total samples	2	23	47	54
Fatigue rates (%)	0	13.04	25.53	83.33

where n is the fatigue life of the specimen, w is the number of failed samples at the same level of life, and k is the total number of failed samples.

The fatigue life of the currently investigated beam specimen lies between 6.1×10^6 and 1.4×10^8 . The results are comparable to a previous study on the use of magnetic loading [17], in that the beam life lay between 1 and 5×10^7 .

CONCLUSIONS

The design, fabrication, and fatigue behavior of a microcantilever beam driven by electrical load is reported in this study. The measurement shows that the deflection increases with both beam length and the load, and the fatigue rate increases correspondingly. For the beam of 60 to 120 μm long, the neck deflection ranges from 61 nm to 460 nm at 150 V and 100 Hz and from 320 nm to 600 nm at 200 V and 100 Hz. The fatigue life lies between 6.1×10^6 and 1.4×10^8 , which is consistent with the early reference of fatigue tests using various loading methods.

ACKNOWLEDGMENT

This research was supported by the National Science Council, Taiwan ROC, under contract NSC92-2212-E007-048.

REFERENCES

- Larsen, K.P.; Rasmussen, A.A.; Ravnkilde, J. T.; Ginnerup, M.; Hansen, O. MEMS device for bending test: measurements of fatigue and creep of electroplated nickel. *Sensors and Actuators A* **2003**, *103*, 156–164.
- Tsuchiya, T.; Tabata, O.; Sakata, J.; Taga, Y. Specimen size effect on tensile strength of surface-micromachined polycrystalline silicon thin films. *Journal of Microelectromechanical Systems* **1998**, *7* (1), 106–113.
- Haque, M.A.; Saif, M.T.A. Microscale materials testing using MEMS actuators. *Journal of Microelectromechanical Systems* **2001**, *10* (1), 146–152.
- Mearini, G.T.; Hoffman, R.W. Tensile properties of aluminum/alumina multi-layered thin films. *Journal of Electronics Materials* **1993**, *22* (6), 623–629.
- Yi, T.C.; Li, L.; Kim, C.J. Microscale material testing of single crystal-line silicon: process effects on surface morphology and tensile strength. *Sensors and Actuators* **2000**, *83*, 172–178.
- Jones, P.T.; Johnson, G.C.; Howe, R.T. Micromechanical structures for fracture testing of brittle thin films. Proc. MEMS, DSC-Volume 59, ASME Int. Mechanical Engineering Congress and Exposition, Atlanta, GA, November 1996, 325–330.
- Yi, T.; Kim, C.J. Measurement of mechanical properties for MEMS materials. *Measurement Science and Technology* **1999**, *10*, 706–716.
- Wilson, C.J.; Ormeggi, A.; Narbutovskih, M. Fracture testing of silicon microcantilever beams. *Journal of Applied Physics* **1996**, *79* (5), 2386–2393.
- Muhlstein, C.L.; Brown, S.B.; Ritchie, R.O. High-cycle fatigue of single-crystal silicon thin films. *Journal of Microelectromechanical Systems* **2001**, *10* (4), 593–600.
- Schwaiger, R.; Kraft, O. Size effect in the fatigue behavior of thin Ag films. *Acta Materialia* **2003**, *51*, 195–206.
- Ando, T.; Shikida, M.; Sato, K. Tensile-mode fatigue testing of silicon films as structural materials for MEMS. *Sensors and Actuators A* **2001**, *93*, 70–75.
- Li, X.D.; Bhushan, B. Fatigue studies of nanoscale structure for MEMS/NEMS applications using nanoindentation techniques. *Surface and Coatings Technology* **2003**, *163–164*, 521–526.
- Muhlstein, C.L.; Brown, S.B.; Ritchie, R.O. High-cycle fatigue and durability of polycrystalline silicon thin films in ambient air. *Sensor and Actuator A* **2001**, *94*, 177–188.
- Kraft, O.; Schwaiger, R.; Wellner, P. Fatigue in thin films: lifetime and damage formation. *Materials Science and Engineering A* **2001**, *319–321*, 919–923.
- Schwaiger, R.; Kraft, O. Size effects in the fatigue behavior of thin Ag films. *Acta Materialia* **2003**, *51*, 195–206.
- Sharpe Jr., W.N.; Bagdahn, J. Fatigue testing of polysilicon—a review. *Mechanics of Materials* **2004**, *36*, 3–11.
- Hocheng, H.; Kao, K.S.; Fang, W.L. Investigation of fatigue of a microcantilever component. *Journal of Vacuum Science and Technology* **2004**, *22* (6), 3143–3146.
- Kovacs, G.T.A. *Micromachined Transducers Sourcebook*; McGraw-Hill: Columbus, OH, 1998.
- Madou, M. *Fundamentals of Microfabrication*; CRC: Boca Raton, FL, 1997.
- Shikida, M.; Sato, K.; Tokoro, K.; Uchikawa, D. Differences in anisotropic etching properties of KOH and TMAH solutions. *Sensors and Actuators* **2000**, *80*, 179–188.
- Steinsland, E.; Finstad, T.; Hanneborg, A. Etch rates of (100), (111) and (110) single-crystal silicon in TMAH measured in situ by laser reflectance interferometry. *Sensors and Actuators* **2000**, *86*, 73–80.
- Chen, P.H.; Peng, H.Y.; Hsieh, C.M. Chyu, M.K. The characteristic behavior of TMAH water solution for anisotropic etching on both silicon substrate and SiO₂ Layer. *Sensors and Actuators* **2001**, *93*, 132–137.